

# VU Research Portal

## Search Space Analysis of Evolvable Robot Morphologies

da Silva Miras de Araujo, K.; Haasdijk, Evert; Glette, Kyrre; Eiben, A.E.

### ***published in***

Applications of Evolutionary Computation - 21st International Conference, EvoApplications 2018, Proceedings 2018

### ***DOI (link to publisher)***

[10.1007/978-3-319-77538-8\\_47](https://doi.org/10.1007/978-3-319-77538-8_47)

[Link to publication in VU Research Portal](#)

### ***citation for published version (APA)***

da Silva Miras de Araujo, K., Haasdijk, E., Glette, K., & Eiben, A. E. (2018). Search Space Analysis of Evolvable Robot Morphologies. In K. Sim, & P. Kaufmann (Eds.), *Applications of Evolutionary Computation - 21st International Conference, EvoApplications 2018, Proceedings* (pp. 703-718). (Lecture Notes in Computer Science (including subseries Lecture Notes in Artificial Intelligence and Lecture Notes in Bioinformatics); Vol. 10784). Springer/Verlag. [https://doi.org/10.1007/978-3-319-77538-8\\_47](https://doi.org/10.1007/978-3-319-77538-8_47)

### **General rights**

Copyright and moral rights for the publications made accessible in the public portal are retained by the authors and/or other copyright owners and it is a condition of accessing publications that users recognise and abide by the legal requirements associated with these rights.

- Users may download and print one copy of any publication from the public portal for the purpose of private study or research.
- You may not further distribute the material or use it for any profit-making activity or commercial gain
- You may freely distribute the URL identifying the publication in the public portal ?

### **Take down policy**

If you believe that this document breaches copyright please contact us providing details, and we will remove access to the work immediately and investigate your claim.

### **E-mail address:**

[vuresearchportal.ub@vu.nl](mailto:vuresearchportal.ub@vu.nl)



# Search Space Analysis of Evolvable Robot Morphologies

Karine Miras<sup>1</sup>(✉), Evert Haasdijk<sup>1</sup>, Kyrre Glette<sup>2</sup>, and A. E. Eiben<sup>1</sup>

<sup>1</sup> Vrije Universiteit Amsterdam, Amsterdam, The Netherlands  
{k.s.m.a.dasilvamirasdearaujo,e.haasdijk,a.e.eiben}@vu.nl

<sup>2</sup> University of Oslo, Oslo, Norway  
kyrrehg@ifi.uio.no

**Abstract.** We present a study on morphological traits of evolved modular robots. We note that the evolutionary search space –the set of obtainable morphologies– depends on the given representation and reproduction operators and we propose a framework to assess morphological traits in this search space regardless of a specific environment and/or task. To this end, we present eight quantifiable morphological descriptors and a generic novelty search algorithm to produce a diverse set of morphologies for any given representation. With this machinery, we perform a comparison between a direct encoding and a generative encoding. The results demonstrate that our framework permits to find a very diverse set of bodies, allowing a morphological diversity investigation. Furthermore, the analysis showed that despite the high levels of diversity, a bias to certain traits in the population was detected. Surprisingly, the two encoding methods showed no significant difference in the diversity levels of the evolved morphologies or their morphological traits.

**Keywords:** Modular robots · Evolutionary Robotics · Morphology  
Generative encoding · Novelty search

## 1 Introduction

Evolutionary Robotics (ER) [1–4] is a field that “aims to apply evolutionary computation techniques to evolve the overall design or controllers, or both, for real and simulated autonomous robots” [3]. Traditionally, the emphasis lies on evolving controllers for fixed robot bodies, but there is a growing interest in evolving the morphologies as well [5–9]. For instance, a generic architecture for a system of embodied on-line evolution of robots in real time and real space was proposed in [10]. However, the current technology of rapid prototyping (3D-printing) and automated assembly is a limiting factor, and studies in simulations remain important.

In this paper we address the issue of morphological diversity in an evolutionary robotic system. In general, there are three essential factors that determine the course of evolution in such a system, (1) the encoding, including the phenotypes

(the set of possible morphologies), the genotypes (the syntactical representation of these phenotypes), and the mapping from genotypes to phenotypes, (2) the reproduction operators that generate new genotypes from existing ones, and (3) the selection operators that depend on the environment and the task at hand. For the sake of this study we distinguish the search space and the application space of an evolutionary robotic system. The search space consists of the encoding and the reproduction operators, while the application space is formed by the environment and the given task. Besides the impact of the environment [11], clearly, the properties of the search space also have a paramount impact of what evolution can achieve. The main research question we address here is: How to investigate the effect of the search space on the set of evolvable morphologies? This question will be broken down into two subquestions:

**Q1:** How to quantify and measure morphological properties?

**Q2:** How to isolate the effects of the encoding and the reproduction from the effects of selection?

The measures and the methodology we propose to answer these questions will be applied to compare a direct encoding and an indirect encoding scheme for the morphological space we work with in our research programme towards physically evolvable modular robots.

## 2 Morphology Space and Morphological Descriptors

Our robot bodies are composed of modules<sup>1</sup> as shown in Fig. 1, based on RoboGen [12]. For this study, the bodies are flat, constructed in 2D, i.e., the modules do not permit attachment on the top or bottom slots, only the lateral ones. Each module type is represented by a letter in the genotype and by a colored block in the visualized phenotype (color indicating the type of block), and any module can be attached to any other through its attachment slots. An arrow inside the block points to the parent module to which the module is attached.

For quantitatively assessing a given modular body we designed and utilized eight morphological descriptors. The maximum number of modules in a robot is limited to  $m_{max}$ . Given an  $m_{max}$ , each descriptor can assume a discrete number of values, and the calculation for these numbers can be found in the accompanying documentation<sup>2</sup>. Each morphological descriptor was normalized to a range between 0 and 1, as explained below.

*Branching.* This descriptor captures how the attachments of the modules are grouped together in the body, and envisions to measure whether the components of the body are more spread or agglomerated. It is defined with Eq. (1):

$$B = \begin{cases} \frac{b}{b_{max}}, & \text{if } m \geq 5 \\ 0 & \text{otherwise} \end{cases} \quad (1)$$

<sup>1</sup> <http://robogen.org/docs/robot-body-parts/>.

<sup>2</sup> <https://tinyurl.com/y9s8ssuc>.

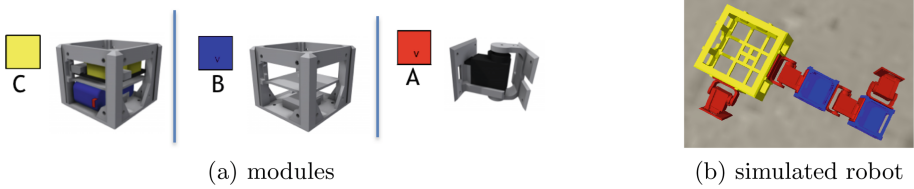


**Fig. 1.** (a) Modules of robots: core-component C holds a controller board; brick B is a cubic module; active hinge A is a joint moved by a servo motor. C and B have attachment slots on its four lateral faces, and A has attachment slots on its two opposite lateral faces; (b) example of a simulated robot.

where  $m$  is the total number of modules in the body,  $b$  the number of modules that are attached on all four faces, and  $b_{max} = \lfloor (m - 2)/3 \rfloor$  – the maximum possible number of modules that can be attached on four faces in a body of  $m$  modules. See Fig. 2 for a few illustrative examples.



**Fig. 2.** Morphology (a) has no module with its four faces attached, (b) has one module with its four faces attached, which is the maximum possible given the size of the body, and (c) has one module with its four faces attached, but could have two, if using the modules indicated by pink arrows to be attached to the one indicated by the orange arrow. (Color figure online)

*Limbs.* This describes the number of extremities of a body:

$$L = \begin{cases} \frac{l}{l_{max}}, & \text{if } l_{max} > 0 \\ 0 & \text{otherwise} \end{cases} \quad (2)$$

$$l_{max} = \begin{cases} 2 * \lfloor \frac{(m-6)}{3} \rfloor + (m - 6) \pmod{3} + 4, & \text{if } m \geq 6 \\ m - 1 & \text{otherwise} \end{cases}$$

where  $m$  is the total number of modules in the body,  $l$  the number of modules which have only one face attached to another module (except for the core-component) and  $l_{max}$  is the maximum amount of modules with one face attached that a body with  $m$  modules could have, if containing the same amount of modules arranged in a different way (Fig. 3).

*Length of Limbs.* Describes how extensive the limbs of the body are and is defined with Eq. (3):

$$E = \begin{cases} \frac{e}{e_{max}}, & \text{if } m \geq 3 \\ 0 & \text{otherwise} \end{cases} \quad (3)$$



**Fig. 3.** Morphology (a) has four modules that could be extremities (considering the limit determined by the size of the body), but only the two indicated by green arrows are; (b) has the maximum number of extremities it could have. (Color figure online)

where  $m$  is the total number of modules of the body,  $e$  is the number of modules which have two of its faces attached to other modules (except for the core-component), and  $e_{max} = m - 2$  – the maximum amount of modules that a body with  $m$  modules could have with two of its faces attached to other modules, if containing the same amount of modules arranged in a different way<sup>3</sup> (Fig. 4).



**Fig. 4.** While in morphology (b) the maximum possible quantity of modules was used as the extension of a limb, in (a), the module indicated by an orange arrow was used as an extra limb. (Color figure online)

*Coverage.* Describes how full is the rectangular envelope around the body. The greater this number, the less empty space there is between neighbor modules. It is defined as Eq. (4):

$$C = \frac{m}{m_{area}} \quad (4)$$

where  $m$  is the total number of modules of the body, and  $m_{area} = m_l * m_w$  – the supported number of modules in the area of the body, with  $m_l$  being the number of modules that would fit in a column as long as the length of the body, and  $m_w$  the number of modules that would fit in a row as long as the width of the body (Fig. 5).



**Fig. 5.** While in morphology (a) all the area created by the body contains modules, in (b), there is space for two more modules.

<sup>3</sup> The types of modules would not have to be necessarily the same, as long as the body had the same amount of modules.

*Joints.* This describes how movable the body is and is defined with Eq. (5):

$$J = \begin{cases} \frac{j}{j_{max}}, & \text{if } m \geq 3 \\ 0 & \text{otherwise} \end{cases} \quad (5)$$

where  $m$  is the total number of modules of the body,  $j$  is the number of effective joints, i.e., joints which have both of its opposite faces attached to the core-component or a brick, and  $j_{max} = \lfloor (m - 1)/2 \rfloor$  – the maximum amount of modules with two opposite faces attached that a body with  $m$  modules could have, in an optimal arrangement (Fig. 6).

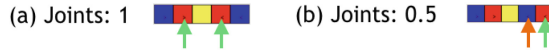


**Fig. 6.** Although both morphologies have two joints, in (b) the second joint is not effective, and would be only if the module indicated by the green arrow was switched with the one indicated by the orange arrow. (Color figure online)

*Proportion.* This describes the 2D ratio of the body and is defined with Eq. (6):

$$P = \frac{p_s}{p_l} \quad (6)$$

where  $p_s$  is the shortest side of the body, and  $p_l$  is the longest side, after measuring both dimensions of length and width of the body (Fig. 7).



**Fig. 7.** Morphology (a) is disproportional and (b) is proportional.

*Symmetry.* This describes the reflexive symmetry of the body with Eq. (7):

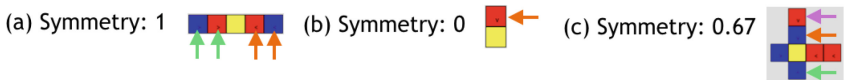


**Fig. 8.** Morphology (a) has the modules indicated by green arrows horizontally reflected by the modules indicated by orange arrows; (b) has no modules reflected; (c) has the module indicated by the orange arrow vertically reflected by the modules indicated by the green arrow, but no reflection for the module indicated by the pink arrow. (Color figure online)

$$Z = \max_{z_v z_h} \quad (7)$$

where  $z_h = o_h/q_h$  – is the horizontal symmetry, and  $z_v = o_v/q_v$  – the vertical symmetry. For calculating each of these symmetry values, a referential center for the body is defined as the core-component. For both horizontal  $h$  and vertical  $v$  axes, a spine is determined as a line dividing the body into two parts according to the center and this axis. Each value is the number  $o$  of modules that have a mirrored module on the other side of the spine (each match of modules accounts for two), divided by the total number  $q$  of compared modules. The spine is not accounted in the comparison (Fig. 8).

*Size.* This describes the extent of the body in terms of number of modules and is defined with Eq. (8):

$$S = \frac{m}{m_{max}} \quad (8)$$

where  $m$  is the total number of modules in the body and  $m_{max}$  the maximum number of modules permitted in any body (Fig. 9).



**Fig. 9.** Morphology (a) is bigger than (b). Example for  $m_{max} = 20$ .

### 3 Exploring the Space of Morphologies

In the foregoing we have introduced eight morphological descriptors that can be used to analyze any given set of robotic morphologies. For instance, they can be measured and plotted during the evolutionary search process and/or applied to assess the final population from a morphological perspective. In this section we demonstrate how they can be used to compare two different representations. To this end, we present a generic methodology for sampling the search space (specified by the encoding and the reproduction operators) independently from the application space (defined by the environment and the task).

The main idea is to create a set of sample morphologies through a *generate-and-test* search process where the *generate* step uses the actual reproduction operators, but the *test* step is based on morphological properties, not influenced by its behavior. The code of our method and the experiments can be found on GitHub<sup>4</sup>.

For these experiments the size of the morphologies,  $m_{max}$ , was limited to 100 modules regardless of the genotype size. Thus, in the body construction phase, after reaching the limit size, extra modules in the genotype were ignored and not included in the phenotype. Additionally, modules which would overlap with other modules were not included in the body. Any morphology generated via crossover or mutation was allowed to lose any part of its genome, except for the mandatory and unique core-component.

<sup>4</sup> <https://tinyurl.com/yc364pfe>.

### 3.1 Encodings

**Generative Encoding:** Our generative encoding represents the genotype of a robot with a Lindenmayer-System (L-System) [9,13], which is a grammatical parallel rewriting system. The grammar of an L-System is defined as a tuple  $G = (V, w, P)$ , where

- $V$ , the alphabet, is a set of symbols containing replaceable and non-replaceable elements
- $w$ , the axiom, is a symbol from which the system starts
- $P$  is a set of production rules for the replaceable symbols

In our design, the symbols of the grammar represent the modules of a robotic body and the commands to assemble them together. The system starts as a simple string of elements and grows to a more complex string iteratively during the rewriting, which performs substitutions of elements through production rules according to a grammar. The alphabet is formed by three letters and two groups of commands as shown in Table 1. For every letter, there is a production rule that might contain any letter or command, and this rule takes place in the rewriting phase to replace its correspondent letter by all of its elements. This representation functions as a developmental process for the genome. Initially, the genome is turned into a single-component structure, the axiom, as the first stage of the L-System. The axiom in this L-System is C (the core-component), and the rewriting process, i.e., development of the genome, iteratively goes on substituting each letter for the items of its production rule. The rewriting results in a string of symbols that straightforwardly maps onto a morphology.

**Table 1.** Alphabet

Symbol	Type	Function
C	module	core-component
B	module	brick
A	module	joint
addr	command	adds the next module to the right of the current one
addl	command	adds the next module to the left of the current one
addf	command	adds the next module to the front of the current one
mover	command	moves the reference to the module to the right of the current
movel	command	moves the reference to the module to the left of the current
movef	command	moves the reference to the module in front of the current
moveb	command	moves the reference to the module behind the current

The decoding of a simple genome is illustrated in Fig. 10a. The genome starts with the axiom C, and for 2 iterations the rewriting rules are performed using the production rules for the replacements. During this construction, a turtle reference



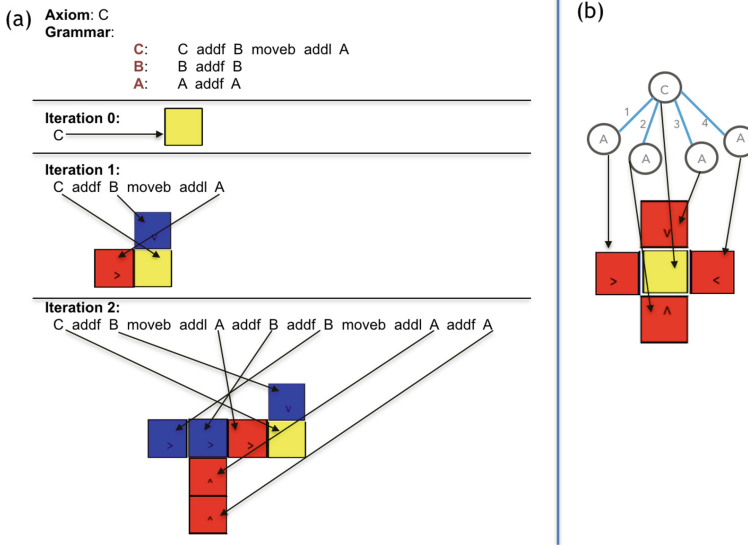


**Fig. 10.** Encoding methods: (a) generative encoding and (b) direct encoding.

is kept for the parser to be localized in the phenotype, which starts at the bottom of the core-component. The turtle reference is updated according to the direction of the new addition movement made. If the current module is a joint, any addition command attaches the new module to the front of it. If all left, front, and right faces of the core-component were occupied, any command of attachment would place a new module to its back. After the replacements, it is possible that some commands end up without a letter in front of it, and in this case the command is a violation and is ignored. Additionally, it is possible that a new module might be supposed to be added in a position where there is a module already. This also generates a violation, and the module is ignored. These violations, which result in ignoring elements of the genotype, can be thought of as non-expressed genes.

**Direct Encoding:** The direct encoding (Fig. 10b) uses a tree-based structure as proposed in [12], and it uses the same modules as the generative encoding. The genotype is composed with one symbol in the tree directly representing each part of the phenotype, and thus, there is a direct genotype-phenotype mapping.

### 3.2 Sampling Algorithm

Our algorithm to generate the set of morphology samples is, in fact, evolutionary. However, selection is based on robot structure, not on robot behavior. We use Novelty Search [14] to maximize the morphological diversity of the sample and to cover a large part of the search space, i.e., find as many different types of morphologies as possible. The corresponding fitness measure is based on the

distance of an individual from the others in a multidimensional space defined by the eight morphological descriptors proposed above. The novelty of an individual  $x$  is calculated as the average distance to its  $k$ -nearest neighbors, where  $k = 15$  and the distance is the Euclidean distance [15] using the morphological descriptors. The set of neighbors for the comparison is formed by the current population, plus an archive, to which every new individual has a 5% probability of being added. The individuals added to the archive remain in it until the end.

Using this novelty objective our evolutionary sampling algorithm was run with a population size of  $\mu = 500$  for 100 generations. In each generation pairs of parents were selected by binary tournament selection,  $\lambda = 250$  offspring were created, and survivors to remain in the population were selected from the set of parents and offspring by 2-tournament selection again. The experiments with each of the two encoding methods were repeated 10 times.

**Reproduction Operators for the Generative Encoding.** The initial random population was created by adding from 1 to 3 random triples of elements to each production rule in the grammar of a genome. A triple was formed by one addition command, one letter and one movement command (Fig. 11a). Crossover of two parents generated one new individual by choosing the production rules randomly from the parents (Fig. 11b). The mutation had 10% of chance of being performed, by choosing a random production rule and applying one of the actions: delete one element in a random position, add one random element in a random position or swap two elements at random positions (Fig. 11c). An exception is made for the production rule of C, which always contains C as its first element, and C cannot be included again, ensuring that a robot has one unique core-component.

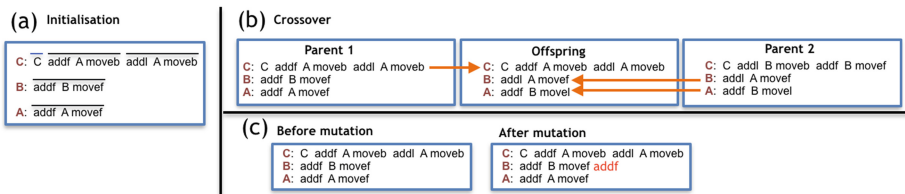


Fig. 11. GE operators.

**Reproduction Operators for the Direct Encoding.** The population was initialized randomly, by adding between 2 and 10 modules to each genome. Crossover was implemented by swapping random subtrees between parents as is standard practice for tree-based genomes (for instance, in Genetic Programming, [16]). Mutations were performed having 10% of chance of applying one of the following the operators: removing a subtree, duplicating a subtree, swapping subtrees, inserting a node or removing a node.

## 4 Results and Discussion

To analyze the morphologies obtained by our evolutionary sampling we use the eight morphological descriptors. The full results are available on Drive<sup>5</sup>.

### 4.1 Individual Morphological Descriptors

In Fig. 12 we see that the search keeps finding new values for all morphological descriptors along the generations. Regarding the distributions of the descriptors, as depicted by Fig. 13, for all of them, the distribution of the values is not uniform, there being a concentration of phenotypes in some values, happening consistently for all runs with both encoding methods. To compare the encoding methods, the descriptors were divided into bins and the frequencies were calculated for the results with both encodings. Table 2 shows correlations for the descriptors ( $p < 0.001$ ), indicating that the concentrations (high frequencies of phenotypes) occur in the same values for both encoding methods. This seems to indicate that there are common regions of attraction, i.e., morphological traits that are more likely to occur, independent of the encoding. Nevertheless, there are other encoding methods in the literature [7, 17], for which we do not know if this result would persist.

**Table 2.** Pearson correlations between the distributions of the descriptors using the two encoding methods. M1 = Branching, M2 = Limbs, M3 = Length of Limbs, M4 = Coverage, M5 = Joints, M6 = Proportion, M7 = Symmetry, and M8 = Size.

M1	M2	M3	M4	M5	M6	M7	M8
0.98	0.95	0.89	0.99	0.98	0.99	0.90	0.98

Some of the concentrations can be explained taking the nature of our system into consideration, such as Branching, Joints, and Symmetry with concentrations in the value 0. This outcome makes sense, because they measure constrained aspects of a morphology. For instance, not all morphologies possess symmetry, while any morphology has a size. The stronger a morphological constraint may be, the harder it may also be for the evolution to find such cases. Coverage, Length of Limbs and Proportion have a concentration in 1, and it is not clear why this happens. By the concentrations of Limbs in 0.5 and Length of Limbs in 1, we see that leg length wins in the tradeoff with the number of limbs.

---

<sup>5</sup> <https://tinyurl.com/ybpcvdqp>.

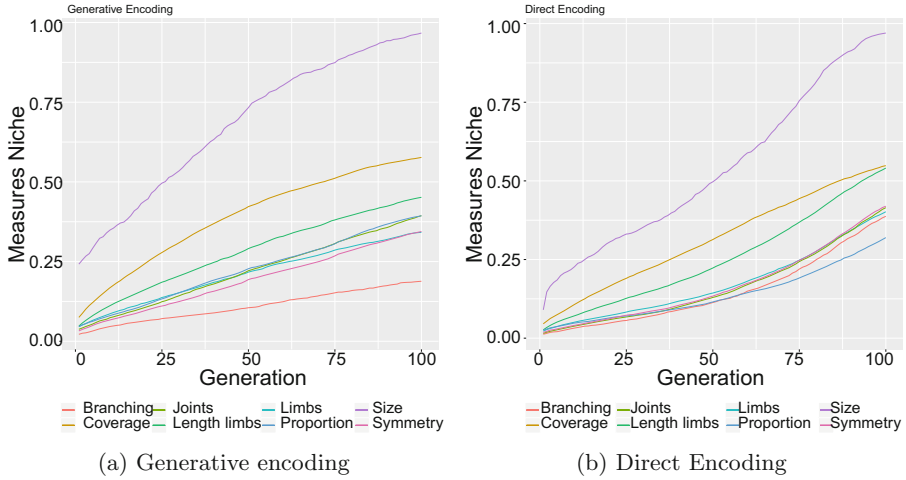


**Fig. 12.** The proportion (average of the runs) of the values discovered for the descriptors, considering the number of all the possible values that the descriptors can assume.

## 4.2 Multidimensional Diversity

To observe the progress of the search for morphological diversity, we define a new measure called Morphological Niche (MN). MN is the number of cubes in the morphological space filled with at least one phenotype, accumulated along the evolutionary run. The grid of cubes was constructed having its dimensions composed of our eight morphological descriptors, each divided into 100 bins of size 0.01 ( $100^8$  cubes in total). Each new phenotype was attributed to its suitable cube, given its morphological descriptors. If the cube had not been filled by any phenotype yet, it accumulated one more point in the MN, otherwise, the number of phenotypes concentrated in that same cube was incremented. In Fig. 14a we see the progression of the MN along the generations, where the values are the averages of the runs. Both methods start with similar values, and the GE surpasses the DE along the generations, but converges to similar values again in the end, presenting no statistically significant difference for the averages of the final MN values. The standard deviations grow along the generations, maybe indicating that the more diverse the population, the more unpredictable the level of diversity of the next generation might be. For both methods, all the MN curves keep on growing linearly along the generations and present growth trend (Mann-Kendall Trend Test  $p < 0.001$ ), suggesting that a longer search will continue to discover new cubes. Notably, the progressive discovery of new cubes may be due not only to the discovery of new values for the individual descriptors, as also to combinations of different discovered values.

As a next step, for each encoding method, we evaluated the density of each point in the multidimensional morphological space, i.e., how many phenotypes found during the search fit the same cube, considering the phenotypes of all

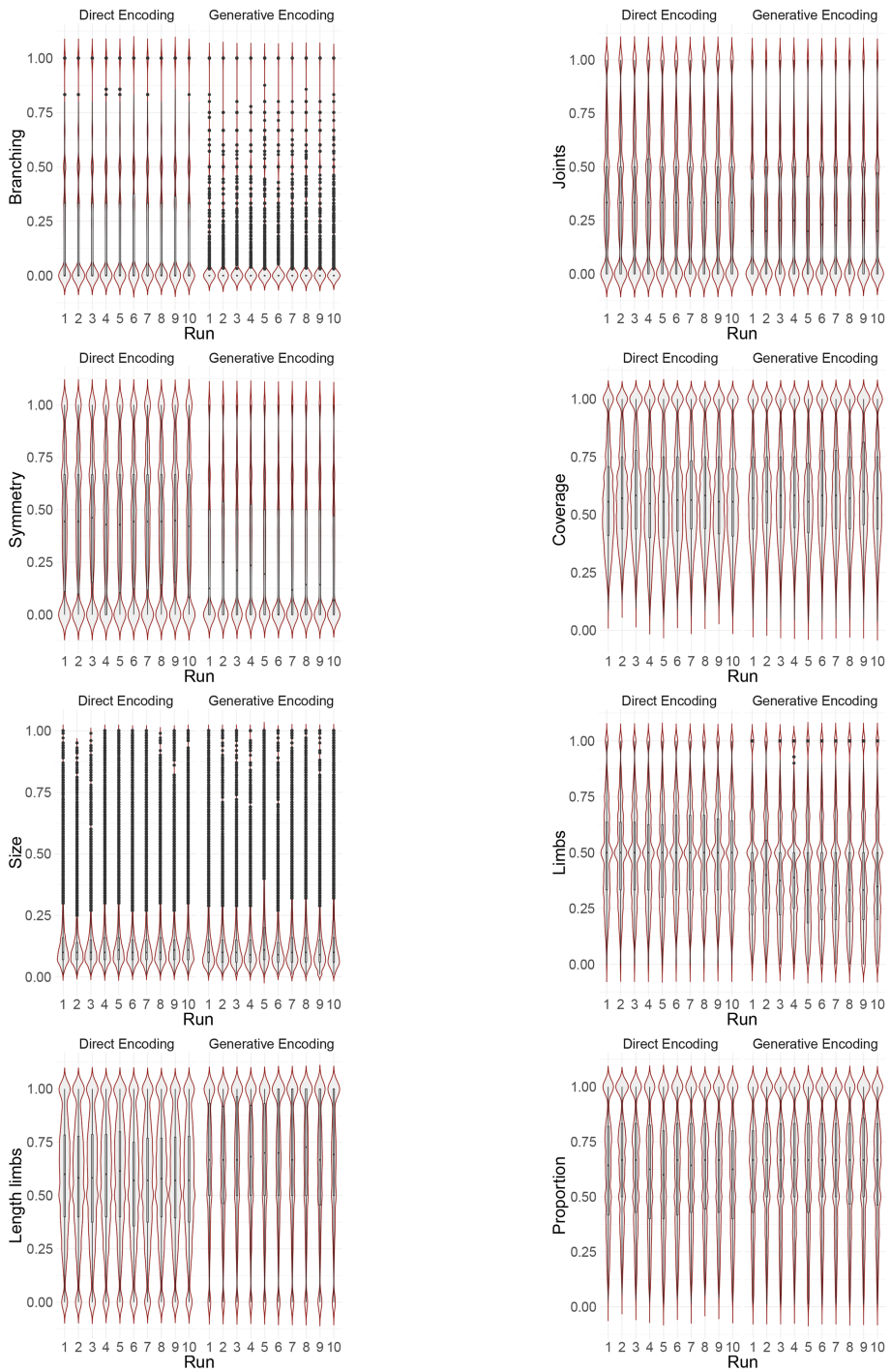
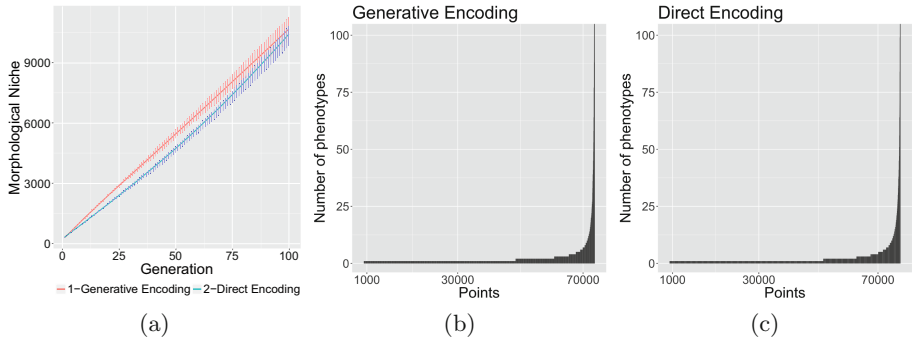


Fig. 13. Violin plots showing the distributions of the descriptors.



**Fig. 14.** (a) Progression of the Morphological Niche along the generations; (b) and (c) Quantity of phenotypes fit in each discovered point of the morphological space over all runs (the graphs were scaled).

runs (Fig. 14b and c). For both encoding methods, we see that occurrences of phenotypes in the same cube of the morphological space are concentrated. The frequencies of phenotypes in the cubes for the individual runs were correlated with each other, showing a significant relation, with Pearson strengths ranging from 0.72 to 0.92 ( $p < 0.01$ ) for all pairs of cases. This shows that for both encoding mechanisms, there is a tendency in discovering certain types of morphologies.

Furthermore, we compared the encoding methods, considering the frequencies of phenotypes in the cubes discovered by them, verifying that there is also correlation (Pearson 0.81,  $p < 0.01$ ). This implies that some types of morphologies are more likely to be found, i.e., there seems to be a bias in morphological traits even without regarding the robot behaviors. Figure 15 shows the most common morphologies, ranked in order from left to right, of each of the runs with both encoding methods. The most common bodies are very similar in all runs, for both encoding methods. These bodies are composed of few modules, mostly from one to four, having frequently one or two limbs, using the extra modules to make limbs a little longer.

This observation could be interesting when analyzing morphological traits of genuinely evolved populations, where robot behavior is taken into account. For instance, one might wonder if the evolved morphological traits are due to the given environment and the nature of the task being performed, or they simply occur because they are more likely to be generated within the used design space. The random initialization and mutations that the system performs could have a tendency to generate some specific types of morphologies, and being aware about it would help one to understand the results of the experiments better.

On the other hand, despite this bias, the morphological diversity of the population is vast, according to the previously mentioned results regarding the MN and values of the descriptors. Figure 16 shows a sample with ten very diverse morphologies found after one evolutionary run.

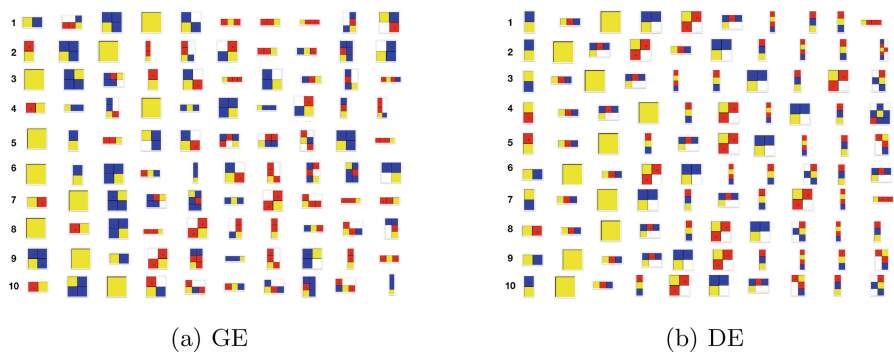


**Fig. 15.** For 10 different runs, the most common discovered morphologies. From left to right, the most common to the least common.



**Fig. 16.** Sample of diverse morphologies found after one evolutionary run.

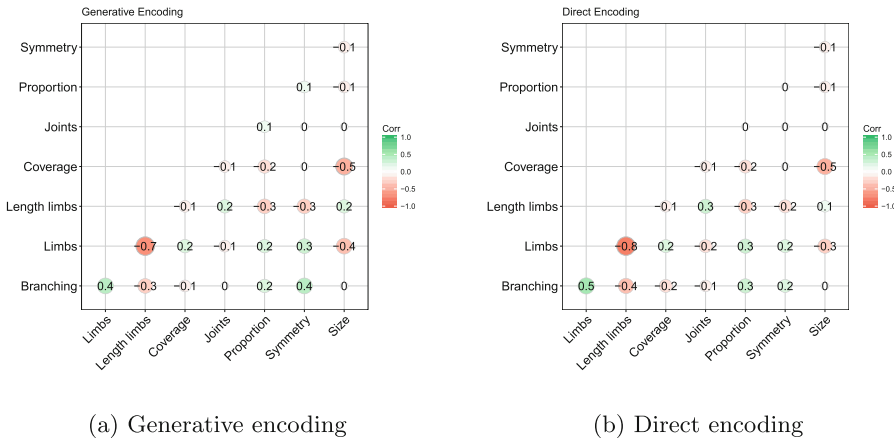


**Fig. 17.** Correlations between descriptors

### 4.3 Relations Between Morphological Descriptors

The correlations between the morphological descriptors are shown in Figs. 17a and b. The data show that most descriptors are not correlated, indicating that morphologies with a wide range of combinations of the values are possible. The exceptions are cases for which the nature of the descriptors is competitive, not permitting some combinations of values. For instance, Limbs and Length of Limbs are negatively correlated because the longer the limbs are, the less there are modules available for new limbs. Size and Coverage are also correlated, as the more modules a body has, there is a higher chance of the extents forming a large rectangular envelope which is hard to fill, thus giving a low coverage score.

## 5 Conclusion and Further Work

This paper presented a framework for assessing the space of possible morphologies within a system of evolving modular robots. The main question was: How to study the properties of (and possible biases in) the search space as defined by the representation and the reproduction operators? To this end we defined eight morphological descriptors and an evolutionary algorithm that sampled the space of possible robots by considering only morphological properties and disregarding behavior. We used Novelty Search and conducted two sets of experiments, each one based on a different representation. The first encoding method was a benchmark direct encoding and the second method was an L-System-based representation, proposed for the purpose of this study.

Our results showed that it is possible to assess morphological diversity utilizing the proposed framework. The resulting morphologies with both encoding methods display a wide range of values for all descriptors. However, we did not observe significant differences in the achieved morphological diversity using each encoding. Furthermore, despite the high diversity achieved, with both methods there are morphological traits that are more commonly found. This indicates that in the utilized design space, a search process is more likely to find some types of morphologies than others. Being aware of such tendencies within a design space could help understand issues related to the morphological traits of evolved populations of robots.

As further work we will add a locomotion task to the fitness of the robots and analyze the impact it will have on the morphological features of the population.

**Acknowledgements.** This project has received funding from the European Unions Horizon 2020 research and innovation programme under grant agreement No. 665347.

## References

1. Nolfi, S., Floreano, D.: *Evolutionary Robotics: The Biology, Intelligence, and Technology of Self-organizing Machines*. MIT Press, Cambridge (2000)
2. Bongard, J.C.: Evolutionary robotics. *Commun. ACM* **56**(8), 74–83 (2013)



3. Vargas, P., Paolo, E.D., Harvey, I., Husbands, P. (eds.): The Horizons of Evolutionary Robotics. MIT Press, Cambridge (2014)
4. Doncieux, S., Bredeche, N., Mouret, J.B., Eiben, A.: Evolutionary robotics: what, why, and where to. *Front. Robot. AI* **2**(4) (2015)
5. Sims, K.: Evolving 3D morphology and behavior by competition. *Artif. Life* **1**(4), 353–372 (1994)
6. Hornby, G.S., Pollack, J.B.: Evolving L-systems to generate virtual creatures. *Comput. Graph.* **25**(6), 1041–1048 (2001)
7. Samuelsen, E., Glette, K., Torresen, J.: A hox gene inspired generative approach to evolving robot morphology. In: Proceedings of the 15th Annual Conference on Genetic and Evolutionary Computation, pp. 751–758. ACM (2013)
8. Corucci, F., Calisti, M., Hauser, H., Laschi, C.: Novelty-based evolutionary design of morphing underwater robots. In: Proceedings of the 2015 Annual Conference on Genetic and Evolutionary Computation, pp. 145–152. ACM (2015)
9. Veenstra, F., Faina, A., Risi, S., Stoy, K.: Evolution and morphogenesis of simulated modular robots: a comparison between a direct and generative encoding. In: Squillero, G., Sim, K. (eds.) *EvoApplications 2017*. LNCS, vol. 10199, pp. 870–885. Springer, Cham (2017). [https://doi.org/10.1007/978-3-319-55849-3\\_56](https://doi.org/10.1007/978-3-319-55849-3_56)
10. Eiben, A., Bredeche, N., Hoogendoorn, M., Stradner, J., Timmis, J., Tyrrell, A., Winfield, A., et al.: The triangle of life: evolving robots in real-time and real-space. *Adv. Artif. Life ECAL* **2013**, 1056–1063 (2013)
11. Auerbach, J.E., Bongard, J.C.: Environmental influence on the evolution of morphological complexity in machines. *PLoS Comput. Biol.* **10**(1), e1003399 (2014)
12. Auerbach, J., Aydin, D., Maesani, A., Kornatowski, P., Cieslewski, T., Heitz, G., Fernando, P., Loshchilov, I., Daler, L., Floreano, D.: Robogen: robot generation through artificial evolution. In: *Artificial Life 14: Proceedings of the Fourteenth International Conference on the Synthesis and Simulation of Living Systems*, pp. 136–137. The MIT Press (2014)
13. Jacob, C.: Genetic L-system programming. In: Davidor, Y., Schwefel, H.-P., Manner, R. (eds.) *Parallel Problem Solving from Nature PPSN III*, pp. 333–343. Springer, Heidelberg (1994)
14. Lehman, J., Stanley, K.O.: Abandoning objectives: evolution through the search for novelty alone. *Evol. Comput.* **19**(2), 189–223 (2011)
15. Lehman, J., Stanley, K.O.: Exploiting open-endedness to solve problems through the search for novelty. In: *ALIFE*, pp. 329–336 (2008)
16. Koza, J.R.: *Genetic Programming: On The Programming of Computers by Means of Natural Selection*, vol. 1. MIT Press, Cambridge (1992)
17. Stanley, K.O., D’Ambrosio, D.B., Gauci, J.: A hypercube-based encoding for evolving large-scale neural networks. *Artif. Life* **15**(2), 185–212 (2009)